Langmuir

ARTICLE

pubs.acs.org/Langmuir

Rapid Microarray Detection of DNA and Proteins in Microliter Volumes with Surface Plasmon Resonance Imaging Measurements

Ting Hu Seefeld, Wen-Juan Zhou, and Robert M. Corn*

Department of Chemistry, University of California-Irvine, Irvine, California 92697, United States

ABSTRACT: A four-chamber microfluidic biochip is fabricated for the rapid detection of multiple proteins and nucleic acids from microliter volume samples with the technique of surface plasmon resonance imaging (SPRI). The 18 mm × 18 mm biochip consists of four 3 μL microfluidic chambers attached to an SF10 glass substrate, each of which contains three individually addressable SPRI gold thin film microarray elements. The 12-element (4 × 3) SPRI microarray consists of gold thin film spots (1 mm^2 area; 45 nm thickness), each in individually addressable 0.5 μL volume microchannels. Microarrays of single-stranded DNA and RNA (ssDNA and ssRNA, respectively) are fabricated by either chemical and/or enzymatic attachment reactions in these microchannels; the SPRI microarrays are then used to detect femtomole amounts (nanomolar concentrations) of DNA and proteins (ssDNA binding protein and thrombin via aptamer−protein bioaffinity interactions). Microarrays of ssRNA microarray elements are also used for the ultrasensitive detection of zeptomole amounts (femtomolar concentrations) of DNA via the technique of RNase H-amplified SPRI. Enzymatic removal of ssRNA from the surface due to the hybridization adsorption of target ssDNA is detected as a reflectivity decrease in the SPR imaging measurements. The observed reflectivity loss is proportional to the log of the target ssDNA concentration with a detection limit of 10 fM or 30 zeptomoles (18 000 molecules). This enzymatic amplified ssDNA detection method is not limited by diffusion of ssDNA to the interface, and thus is extremely fast, requiring only 200 s in the microliter volume format.

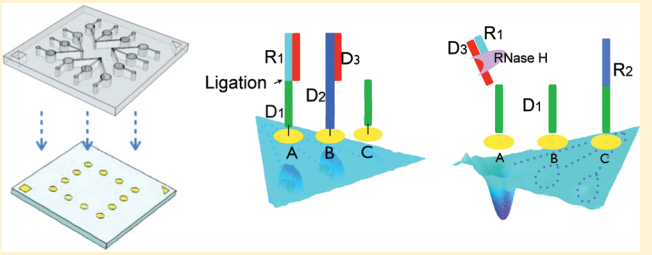

I. INTRODUCTION

The detection and identification of DNA, RNA, and proteins by bioaffinity adsorption onto oligonucleotide microarrays has many applications in the areas of biology, biotechnology, and medicine.[1−4] Some of these applications require the detection of a small number of molecules from microliter volume samples, from femtomoles (nanomolar concentrations) down to zeptomoles (femtomolar concentrations). Examples include the early detection of colorectal cancer and cervical cancer from clinical DNA samples[5−7] and the detection of microRNA (miRNA) for profiling gene expression.[4,8,9] Additionally, the early diagnosis of diseases from clinical samples would benefit from the rapid detection and quantification of small numbers of protein biomarker molecules in microliter volumes, and research efforts such as the study of populations of genetically identical cells will require the detection and quantification of very small amounts of regulatory proteins.[7]

The technique of surface plasmon resonance imaging (SPRI) has been shown to be an extremely versatile platform for the multiplexed detection and quantitation of biomolecules via microarray measurements of surface bioaffinity interactions.[10,11] For example, SPRI microarray measurements have been used previously to measure nucleic acid hybridization,[12] protein−DNA binding,[13,14] protein−antibody binding,[15] and carbohydrate-lectin binding[16] at target molecule concentrations that are typically at or above 1 nM. To detect even lower concentrations of biomolecules with SPRI, a number of nanoparticle-based and surface enzyme-based signal amplification schemes have been implemented.[17−25] For example, we have previously shown that the method of RNase H-amplified SPRI can be used to detect single-stranded DNA (ssDNA) down to a concentration of 10 fM.[26,27] However, all of our previous studies have been performed with milliliter samples in a circulating flow cell format that creates a steady state concentration gradient from solution to the surface.[12,28]

In this paper, we develop and demonstrate a stationary microliter volume format for SPRI that can be used to detect small amounts (femtomoles to zeptomoles) of relevant nucleic acid and protein biomarkers. Specifically, we create biochips that consist of four 3 μL PDMS microfluidic trichannel chambers attached to an SF10 glass substrate that each contain three individually addressable SPRI gold thin film (1 mm^2 area; 45 nm thickness) microarray elements. A diagram and picture of this microchamber biochip are shown in Figure 1. A 12-element (4 × 3) SPRI biomolecular microarray is fabricated directly in the microchamber biochip by separate surface attachment reactions that occur in 12 individually addressable 0.5 μL subvolume microchannels. A combination of chemical attachment and surface enzymatic attachment reactions are used to create

Received: February 18, 2011
Revised: March 29, 2011
Published: April 13, 2011

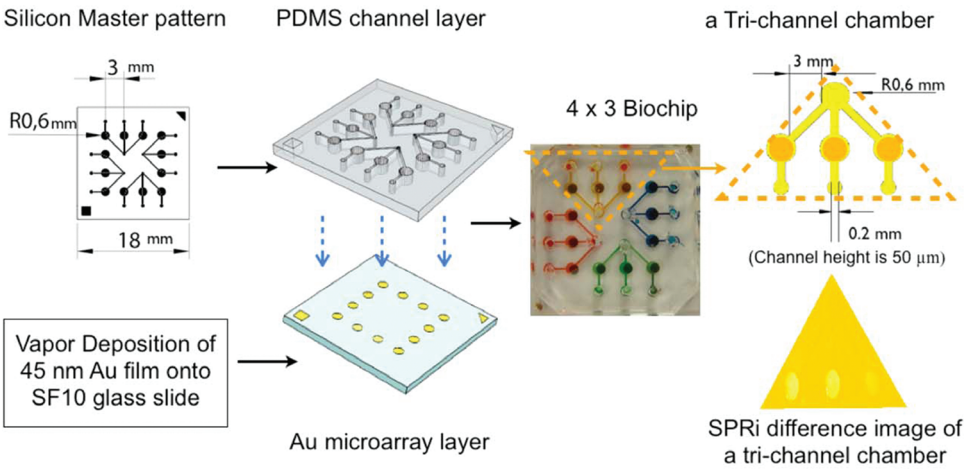

Figure 1. Schematic representation of the small volume biochip engineering.

Table 1. DNA and RNA Sequences

symbol	sequence
Dt	5′-TTTTTTTTTTTTTTTTTTTTTTTTTTTTTT-NH2-3′
Da	5′-AGTCCGTGGTAGGGCAGGTTGGGGTGACTTTTTTT-TTTTTTTTT-NH2-3′
D1	5′-PO_4-GAGTTGCTGCTTATGT-NH_2-3′
D2	5′-CGTGCCACCCTTTTCCCCAGGAGTTGCTGCTTATGT-NH_2-3′
D3	5′-CTGGGGAAAAGGGTGGCACG-3′
R1	5′-CGUGCCACCCUUUUCCCCAG-3′
R2	5′-AUAGAAAUUGACAAGGGAGG-3′

ssDNA and single-stranded RNA (ssRNA) microarrays.[17,29] After array fabrication, the microchannels are flushed out with buffer solution, and then four separate 3 μL target volumes are introduced into the microchambers of the biochip. Real-time SPRI measurements are used to monitor the specific adsorption of ssDNA and two proteins, ssDNA binding protein (SSB) and thrombin, onto the microarray elements from quiescent nanomolar solutions. Microarrays of ssRNA are also used for the ultrasensitive detection of ssDNA at femtomolar concentrations (corresponding to zeptomoles of sample) via the technique of RNase H-amplified SPRI.[26,27] The observed reflectivity loss is proportional to the log of the target ssDNA concentration with a detection limit of 10 fM or 30 zeptomoles (18 000 molecules). This enzymatic amplified ssDNA detection method is extremely fast, requiring only 200 s in the microliter volume format. The unique speed of these measurements derives from the fact that they neither require the buildup of a measurable amount of adsorbed ssDNA nor result in the depletion of target ssDNA in solution.

II. EXPERIMENTAL CONSIDERATIONS

Materials. 11-Amino-1-undecanethiol hydrochloride (MUAM; Dojindo), poly-L-glutamic acid (MW = 2000−15 000; pGlu; Sigma), 1-ethyl-3-(3-(dimethylamino)propyl)carbodiimide hydrochloride (EDC; Pierce), *N*-hydroxysulfosuccinimide (NHSS; Pierce), ethanol (Gold Shield, absolute), urea (Sigma-Aldrich), polydimethylsiloxane (PDMS) curing agent and Sylgard 184 Silicone elastomor (Dow Corning) were used as received. T4 RNA Ligase (Promega), polyethylene glycol (PEG; Promega), RNasin Ribonuclease Inhibitor (Promega), RNase H and RNase H buffer (New England Biolabs), α-Thrombin protein (Haematologic Technologies) and SSB (Epicenter Biotechnologies) were used as received. DNA oligonucleotides were received from Integrated DNA Technologies (IDT), and RNA oligonucleotides were received from Dharmacon RNAi Technologies and used as received. All DNA and RNA used were high-performance liquid chromatography (HPLC) purified and desalted. A phosphate -buffered saline (PBS) buffer (100 mM Na_2HPO_4, 0.3 M NaCl, 5 mM $MgCl_2$, 1 mM EDTA, adjusted to pH 7.4) was used for all DNA array fabrication. The DNA and RNA sequences used are summarized in Table 1. All the DNA and RNA sequences were checked using IDT OligoAnalyzer 3.1 folding calculations and showed no hairpin formation at room temperature.

Microfluidic Biochip Assembly. An 18 × 18 mm microfluidic biochip with 4 × 3 channels was assembled by the attachment of a SF10 glass onto a PDMS channel layer as shown in Figure 1. Twelve gold film spots (1 mm diameter, 45 nm thickness) with 1-nm underlayer of chromium were deposited onto SF10 glass (Schott Glass, 18 × 18 mm) using a Denton DV-502A metal evaporator. The PDMS layer with 4× trichannels (50 μm height and 200 μm width channel) was created by replication from a 3D silicon master using standard soft lithography procedures. After being peeled off from the master, the PDMS layer was trimmed, and the inlets and outlets were individually punched with a 1.2 mm diameter needle. The PDMS layer was then sonicated in ethanol and water for 10 min, respectively, to remove any impurity from the PDMS surface. After drying with N_2, the SF10 glass and PDMS layer were both treated in a plasma oxidation chamber then covalently bonded together to form the assembled biochip.

DNA Microarray Fabrication. DNA microarrays were fabricated in situ in the microchannel biochip using a surface attachment chemistry adapted from previous publications.[17] The assembled biochip was immersed in a 1 mM ethanolic MUAM solution for at least 12 h. After rinsing each chamber with ethanol, water, and drying with N_2, 0.5 μL of PGlu (3 mg/mL) in PBS buffer was injected onto each microarray element and incubated at room temperature for 1 h to form an electrostatically adsorbed pGlu monolayer on the amino-terminated MUAM. After a second rinsing and drying step, 0.5 μL of 200 μM 3′-amine modified and 5′-phosphorylated ssDNA solution in a PBS buffer that contained

dx.doi.org/10.1021/la200649n |*Langmuir* 2011, 27, 6534–6540

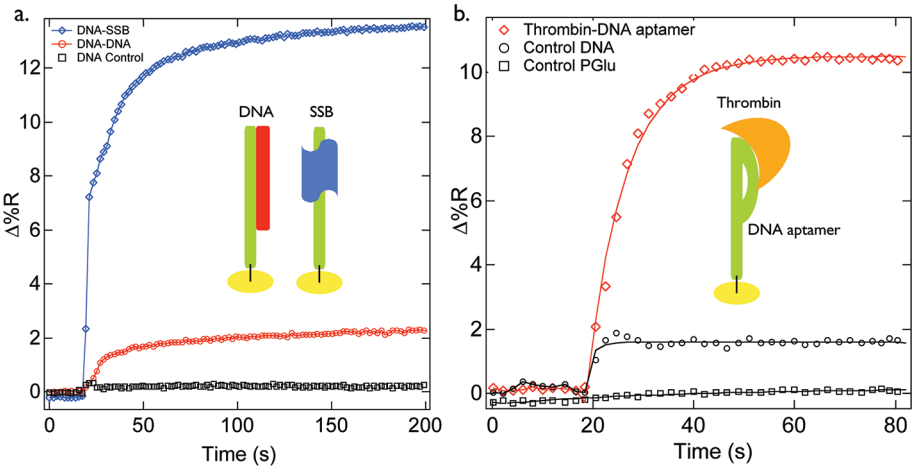

Figure 2. (a) Real-time SPRI kinetic measurements of DNA and SSB protein detection with ssDNA microarray elements on a small volume biochip. (b). Real-time SPRI kinetic measurements of Thrombin protein detection with DNA aptamer microarry elements on a small volume biochip.

75 mM EDC and 15 mM NHSS was injected onto each microarray element and incubated at room temperature for at least 24 h to covalently link the DNA to the pGlu and the pGlu to the MUAM monolayer.

Enzymatic Surface RNA Ligation. RNA microarrays were fabricated by first creating the 5′-phosphorylated ssDNA microarray elements, then attaching unmodified ssRNA molecules onto the ssDNA monolayer with a T4 RNA ligase surface ligation reaction procedure adapted from our previous publications.[23,29] The microarray elements were exposed to the ssRNA and RNA ligation buffer solution for at least 24 h at room temperature, followed by rinse steps of 8 M urea and then water to remove any enzyme and unattached ssRNA from the chambers.

RNA Ligation Buffer Solution. The ssRNA ligation solution contained 200 μM unmodified ssRNA in a ligation buffer (50 mM Tris, 10 mM $MgCl_2$, 5 mM dithiothreitol (DTT), and 1 mM adenosine-5'-triphosphate (ATP), pH 7.8), T4 RNA ligase (0.25 U/μL), RNasin RNase inhibitor (0.05 U/μL), and 20% (w/v) PEG.

RNase H Buffer Solution. An RNase H buffer solution contained a RNase H reaction buffer (75 mM KCl, 50 mM Tris-HCl, 3 mM MgCl2, 10 mM Dithiothreitol, pH 8.3), and RNase H (0.06 U/μL) for all of the RNase H experiments.

SPRI Measurements. All the SPRI measurements were performed on a SPRimager from GWC Technologies (Madison, WI).

III. RESULTS AND DISCUSSION

A. Design and Fabrication of the Four Sample Trichannel Microchips. In order to detect nucleic acids and proteins in microliter sample volumes, we constructed a special multichannel small volume microchip format for SPRI measurements. A microchip of four trichannel chambers was created in PDMS using a previously described Silicon 3D master soft lithography technology[30] and then attached to an 18 mm × 18 mm SF10 glass substrate; this microchip is denoted as a "4 × 3 biochip" (Figure 1). Each trichannel chamber contained three microarray elements (45 nm gold thin film spots with 1 mm diam.), and each microarray element was in a separate subchannel with its own delivery port to be used during microarray fabrication. Each separate subchannel could be filled with 0.5 μL of an attachment chemistry solution, rinsed, dried, and then refilled with additional attachment chemistry solutions as necessary. Further details of the fabrication procedures are described in the Experimental Considerations.

After completion of the array fabrication process, the biochip was simultaneously exposed to four different 3 μL target solutions through the connected delivery inlets of the trichannel chambers (see Figure 1). This "4 × 3" design allowed us to perform four separate three-element SPRI microarray measurements simultaneously on one biochip, each with a total stationary target volume of 3 μL. In comparison, the microfluidic cell we have used previously for SPRI microarray measurements typically required 1−5 mL of target solution and could only analyze one target solution at a time. Targets solutions on the microchannel biochip were introduced via simple pipetting, thus avoiding the need for any microfluidic flow tubing and pumps. The width and height of the microchannels (200 and 50 μm respectively) was optimized to prevent cross-channel contamination during array fabrication while still permitting bubble-free injection and effective rinsing during the assay process. Additionally, the design of this small volume microchannel biochip allowed for the reaction elements to be completely sealed inside the PDMS chamber, eliminating any possible airborne contamination during fabrication and the course of SPRI measurements.

B. DNA Microarray Fabrication and Biosensing. As a first demonstration of the utility of the microchip format for SPRI measurements, biochips containing ssDNA and DNA aptamer microarrays were fabricated and used in a series of bioaffinity adsorption experiments. Exemplary real-time SPRI kinetic curves obtained from the detection of DNA on ssDNA microarray are shown in Figure 2a. SPRI adsorption curves obtained from 3 μL of a 1 μM solution of a ssDNA 20mer (Sequence D3 in Table 1) onto a complementary ssDNA microarray element (Sequence D2) and a noncomplementary control DNA microarray element (Sequence D1) are plotted in Figure 2a as circles and squares, respectively. A final reflectivity change (Δ%R) of 2% was observed for the complementary microarray element; this value indicates the formation of a full double-stranded DNA (dsDNA) monolayer.[17] Negligible reflectivity change was observed for the noncomplementary microarray element, verifying that there was negligible amount of nonspecific adsorption onto the ssDNA microarray elements.

Also shown in Figure 2a is an SPRI adsorption curve (diamonds) from a second experiment with a ssDNA microarray

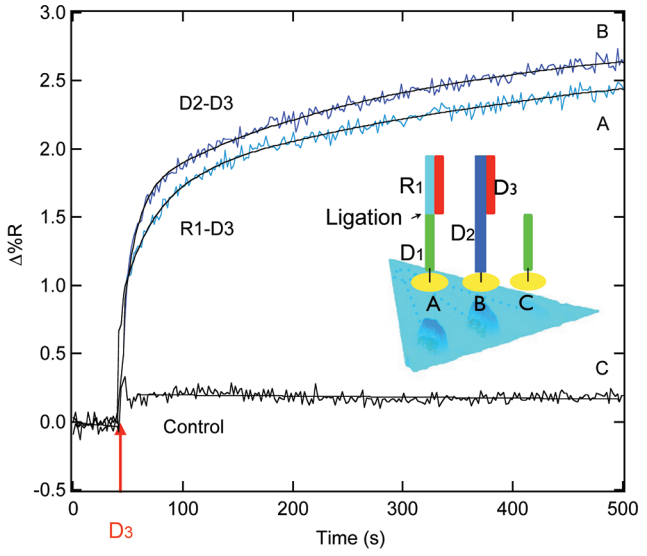

Figure 3. Real-time SPRI kinetic measurements of the T4 enzymatic RNA ligation efficiency of RNA microarrays in a trichannel chamber.

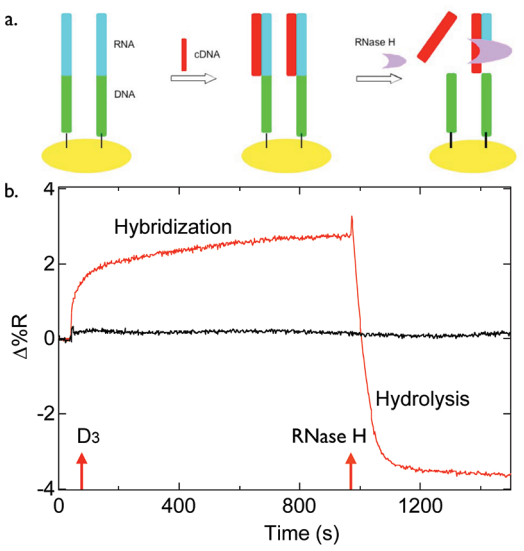

Figure 4. Real-time SPRI measurements of the two-step hybridization−hydrolysis experiments to test the RNase H enzymatic activity on T4 ligated RNA microarrays. Arrows indicate the introduction of target ssDNA (D3) solution and RNase H solution.

biochip in which the target solution consisted of 3 μL of a 30 nM solution of SSB. SSB specifically adsorbs onto ssDNA;[31] since it is a protein with a MW of 75 KD, a larger steady-state SPRI reflectivity change of 13% was observed. This value of the reflectivity change is comparable to that achieved previously in milliliter circulating flow cell format SPRI experiments.[17] Even at 30 nM, this SSB adsorption process reached 90% completion in approximately 100 s. The final steady-state SPRI reflectivity change depended on both the solution concentration and the Langmuir adsorption coefficient.[22] As the SSB target concentration was lowered to 3 nM, the steady-state SPRI reflectivity change decreased to 4%, again reaching 90% completion in approximately 100 s (data not shown). These values are consistent with the K_{ads} of 5×10^9 M^{-1} reported previously.[17] No decrease in adsorption rate due to either diffusion or stoichiometric limitations was ever observed for SSB or DNA adsorption in the 3 μL microchip format.

Figure 2b shows the SPRI adsorption curves from an experiment on a DNA aptamer microarray biochip that consisted of three microarray elements: a DNA thrombin aptamer sequence (Sequence Da), a DNA T_{30} control sequence (Sequence Dt), and a pGlu-MUAM monolayer. Aptamers are oligonucleotides (either ssDNA or ssRNA) that can fold into specific configurations and noncovalently bind with a specific protein; aptamers have many industrial and clinical applications such as macromolecular drug candidates, proteomic microarrays and medical diagnostics.[32] The ssDNA sequence Da has been used as an aptamer that binds to the biologically relevant biomarker protein thrombin.[33] Figure 2b shows the SPRI reflectivity curve (red diamonds) of thrombin adsorption onto this aptamer sequence (target solution: 3 μL total volume, 180 nM thrombin concentration). Also shown in Figure 2b is a weak thrombin adsorption onto the control DNA element sequence. This weaker adsorption onto the Dt sequence was distinguished by a fast dissociation and reflectivity loss upon introduction of a buffer solution (data not shown). Also shown in Figure 2b is the SPRI reflectivity from the pGlu−MUAM microarray element, which shows no thrombin adsorption. These measurements clearly demonstrate that the small stationary volume biochip format can be used to rapidly detect microliter protein biomarkers at nanomolar concentrations with aptamer microarrays.

C. RNA Microarray Fabrication and Characterization. In a second set of experiments, we have demonstrated that bioactive ssRNA microarrays can be enzymatically fabricated and manipulated in situ in the quiescent small volume microchip format. Microarray elements of ssRNA were created on the gold spots using a two-step process: first, 5′-phosphorylated ssDNA was attached to the gold surface microarray elements, then ssRNA was attached to the surface ssDNA microarray by a ligation reaction using the enzyme T4 RNA ligase.[23,29]

To confirm the formation of the ssRNA microelements and measure the efficiency of the T4 RNA surface ligation reaction in the biochip format, the RNA microarrays were characterized with the hybridization adsorption SPRI kinetics measurements shown in Figure 3. As shown schematically in the Figure 3 inset, the three microarray elements in a trichannel set consisted of (A) a 5′-phosphorylated ssDNA element (anchor sequence D1) onto which ssRNA was enzymatically ligated (20mer probe sequence R1, a human miRNA sequence randomly chosen from miRNA database miRBase, ID# hsa-miR-1227, Accession MI0006316), (B) an ssDNA element with a anchor probe DNA sequence (D2), where D2 sequence is equivalent to the RNA sequence R2 plus anchor sequence D1, and (C) a control ssDNA element that only contained the D1 anchor sequence. Three microliters of a 1 μM ssDNA solution (sequence D3, which is complementary to both R1 and partially D2) was introduced into the microfluidic chamber; the real time SPRI reflectivity curves obtained from the three microarray elements are shown in Figure 3. As expected, two of the three microarray elements (A and B) show an increase in reflectivity due to the hybridization of the target DNA (D3) onto the surface (this process is denoted as "hybridization adsorption"). The SPRI reflectivity curve from the microarray element undergoing DNA−DNA (D2−D3) hybridization adsorption resulted in an SPRI reflectivity change (Δ%R) of 2.7 ± 0.1%, whereas the reflectivity curve from the microarray element undergoing RNA−DNA (R1−D3) hybridization adsorption

dx.doi.org/10.1021/la200649n |*Langmuir* 2011, 27, 6534–6540

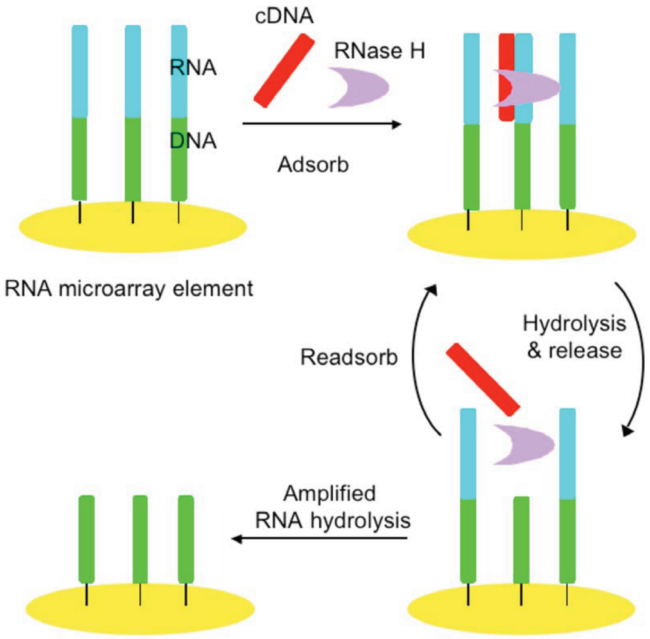

Figure 5. Schematic representation of RNase H surface enzymatic amplification for the ultrasensitive detection of ssDNA on microarray format.

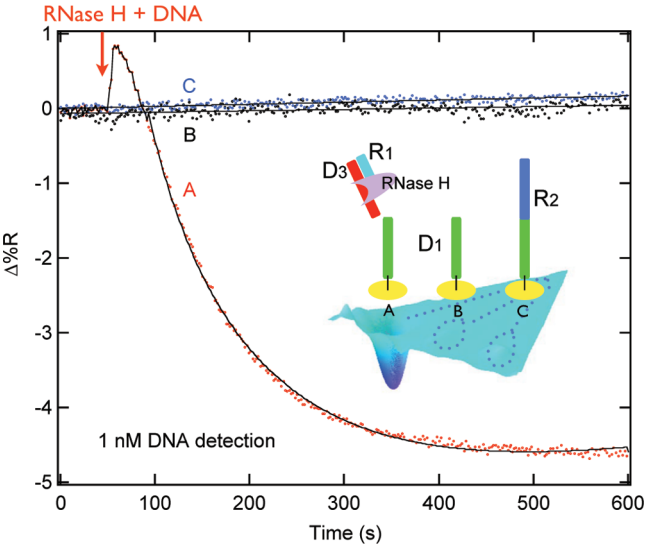

Figure 6. Real-time SPRI kinetic measurements of the RNase H amplified detection of 1 nM ssDNA target solutions. The scheme inset represents the SPR difference image from a trichannel chamber and its corresponding surface chemistry.

resulted in a Δ%R of 2.4 ± 0.1%. Assuming similar surface hybridization efficiencies, we can estimate the RNA−DNA T4 surface ligation efficiency to be 90 ± 5%. The SPRI data from control element C exhibited negligible hybridization adsorption (only a small (0.2%) reflectivity increase just after injection of the target DNA that we attribute to a very small bulk refractive index change). A three-dimensional representation of the SPRI difference image for the trichannel chamber obtained after hybridization adsorption is also shown as an inset in Figure 3.

To verify that the ssRNA microarray elements were available for further surface enzymatic reactions in the small volume format, a two-step experiment was performed as shown schematically in Figure 4a. RNase H is an enzyme that specifically hydrolyzes RNA in an RNA−DNA heteroduplex.[34,35] In this experiment, the hybridization adsorption of DNA onto the RNA microarray is followed by an RNase H hydrolysis reaction of the surface-bound heteroduplexes. The SPRI reflectivity curves from this experiment are shown in Figure 4b. As in the previous hybridization adsorption measurements, an ssRNA (R1) microarray element was first exposed to a solution containing complementary target DNA (D3), resulting in a Δ%R increase due to the formation of RNA−DNA heteroduplexes on the surface. A buffer solution containing RNase H was then introduced into the trichannel chamber; RNase H specifically adsorbed onto this heteroduplex and then selectively hydrolyzed the RNA. This RNA hydrolysis also released the target DNA from the surface, resulting in a loss of reflectivity corresponding to approximately twice the increase observed during the adsorption of the DNA to the surface. These experiments confirm that (i) enzymatic ligation surface attachment chemistry of ssRNA can be used to create ssRNA microarray elements in the small volume microchip format, and (ii) these ssRNA microarray elements are bioactive and can be hydrolyzed by RNase H after DNA hybridization adsorption from solution to form surface-bound RNA−DNA heteroduplexes. This surface RNase H hydrolysis will be used in the next section to enhance the detection of DNA with SPRI.

D. Zeptomole Detection of DNA in Microliter Volumes with RNase H-Amplified SPRI. Having shown that bioactive DNA and RNA microarrays can be created in the small volume microchip format, these microchips were used to rapidly detect extremely small concentrations of DNA with the technique of RNase H-amplified SPRI. In this experiment, DNA is detected by using RNA microarrays in the presence of the enzyme RNase H as shown schematically in Figure 5. When a solution containing both RNase H and a very small amount of target ssDNA was introduced to ssRNA microarray elements, the surface hydrolysis process starts as soon as there are RNA−DNA heteroduplexes on the surface. Most importantly, the target DNA that was released from the RNA hydrolysis reaction can subsequently rehybridize with another ssRNA on the surface, and lead to a repeated adsorption−hydrolysis amplification reaction cycle.[26,27,36] A very small number of ssDNA molecules can remove a large fraction of the ssRNA from the surface, which will be detected as a decrease in SPRI reflectivity. This method has been used in a milliliter volume circulating flow cell format to detect ssDNA down to a concentration of 10 fM.[26,27] It is a very high fidelity signal amplification strategy with very few false positives because the RNase H amplification chemistry requires a new sequence-specific target binding event (RNA−DNA surface heteroduplex formation) for each cycle of amplification.

A first example of using this RNase H amplified SPRI detection method in a stationary small volume microchip format is shown in Figure 6. As shown in the figure inset, the three-component microarray consisted of two RNA microarray elements (A and C, sequences R1 and R2, respectively), and one DNA microarray element (B, sequence D1). Three microliters of a target solution that contained both 1 nM ssDNA (Sequence D3, which is complementary to R1, but not R2 or D1) and RNase H was introduced into the microchip, and the SPRI kinetic curves in Figure 6 were obtained. A large loss in reflectivity (−4.6% after 600s) was observed for microarray element A due to the hydrolysis of surface-bound RNA−DNA heteroduplexes. This large reflectivity decrease is due to the complete removal of

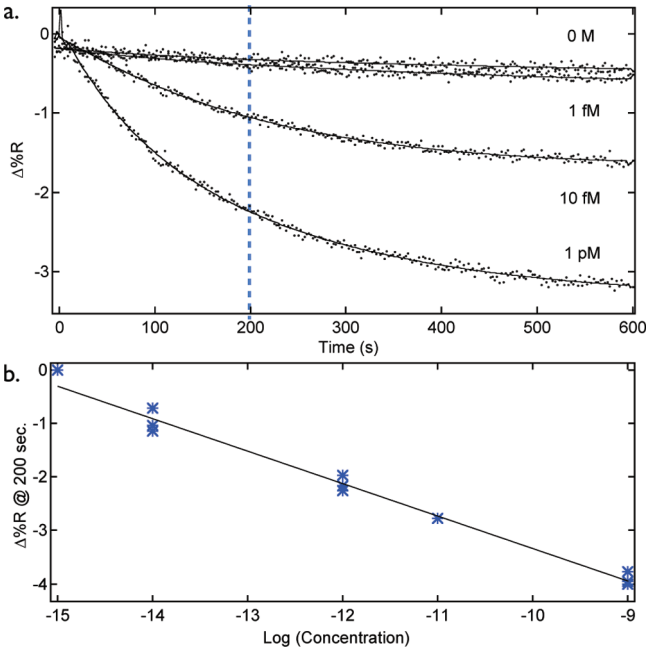

Figure 7. (a) Real-time SPRI kinetic measurements of the RNase H amplified detection of ssDNA target solutions from 0 M to 1 pM. (b) Plot of Δ%R at 200 s after target injection vs log (DNA concentration).

ssRNA from the array element surface.[36] The two control elements showed no loss or gain in signal, demonstrating the absence of both nonspecific adsorption and, most importantly, RNase A contamination, which, if present, would hydrolyze all surface ssRNA microarray elements without any heteroduplex formation. Also shown in the inset of Figure 6 is a three-dimensional representation of the SPRI difference image of the trichannel chamber after exposure to RNase H and target DNA. The three-dimensional SPRI difference image of the trichannel chamber after the hydrolysis are also shown in Figure 6 inset.

Figure 7 shows a series of real-time SPRI kinetic measurements obtained from the RNase H amplified detection of 3 μL ssDNA target solutions with concentrations of 0 M, 1 fM, 10 fM, and 1 pM. A measurable decrease in reflectivity is seen for all solutions with a concentration of 10 fM ssDNA or higher. As observed in previous RNase H-amplified SPRI measurements in milliliter flow cell formats, the initial slope of the decrease varied logarithmically with target DNA concentration.[26,27] This logarithmic dependence can be quantitated by plotting the normalized Δ%R loss at 200 s versus the log of the DNA concentration as shown in Figure 7b. A straight line is observed with a lower limit intercept at approximately 1 fM; this logarithmic dependence suggests that the ssDNA concentration controls the rate of RNase H hydrolysis.

In Figure 6, a small transient increase in reflectivity (Δ%R = +0.8%) was also observed on element A immediately after injection and prior to the reflectivity decrease mentioned previously. This small increase after injection is attributed to the simultaneous adsorption of ssDNA and RNase H enzyme onto the ssRNA microarray element surface. At all concentrations below 100 pM, the transient increase after injection is not observed, and only a monotonic decrease in reflectivity is observed. This is attributed to the fact that at these lower concentrations, the number of ssDNA−RNase H complexes adsorbed to the surface is very small. In fact, the *total* number of

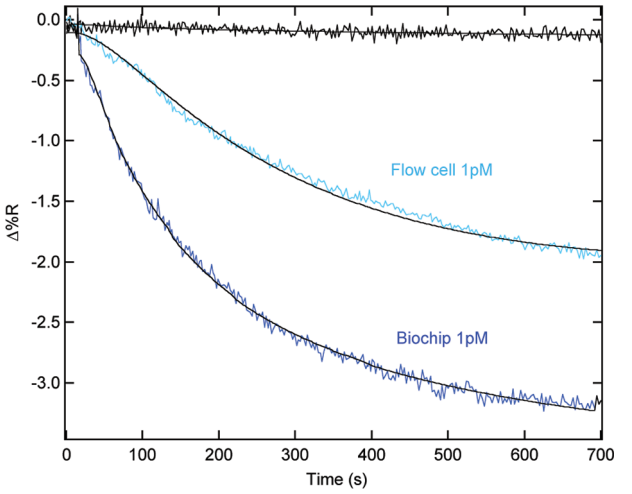

Figure 8. RNase H-amplified SPRI measurements for a 1 pM sample on both the small volume microliter biochip format and milliliter circulating microfluidic cell format.

ssDNA molecules in the sample is small: 3 μL of a 10 fM ssDNA solution corresponds to 18 000 molecules or 30 zmol.

Why is this ultrasensitive detection methodology so rapid? A key advantage of this technique is that the signal does not depend on the accumulation of surface-bound DNA. The DNA adsorbs, cuts RNA, and then is released back into solution. A concentration gradient is not formed at the interface since there is no depletion of solution DNA, and the overall concentration of DNA in solution is not altered. This makes the technique limited only by the speed of the RNase H hydrolysis process on the surface, which is in contrast to any surface bioaffinity sensing method that requires a build up a measurable surface concentration of adsorbed target molecules.[20,25,37,38] Those methods can take very long times (up to hours for femtomolar concentrations of DNA) to build up a detectable signal level due a number of factors: (i) the diffusion rate of target molecules to the interface, (ii) the surface bioaffinity adsorption kinetics, and (iii) the equilibrium surface concentration as determined from the Langmuir adsorption coefficient.[22,39−41]

Further evidence that the microchip format is uniquely suited for RNase H amplified SPRI measurements is shown in Figure 8. In this figure, RNase H-amplified SPRI measurements for a 1 pM target DNA sample are shown both for the microliter biochip format and milliliter flow cell format. The loss of signal due to surface hydrolysis is faster in the quiescent microchip format. We attribute this enhanced loss to the participation of a larger number of solution target DNA in the hydrolysis process in the microchip format. In the small volume microliter biochip format, a significant fraction of the DNA in the microchannel can continuously interact with the surface (the channel height is only 50 μm, so that diffusion across the entire channel can occur within a few seconds, assuming a DNA diffusion coefficient of 10^{-6} cm^2 s^{-1}).[42,43] In contrast, the microfluidic flow format constantly sweeps target molecules in the microchannel away from the array surface, so that only a smaller number of molecules can interact with the surface at any given instant.

IV. CONCLUSIONS

In this paper we have presented a novel small volume microfluidic chip format for detecting DNA and proteins from microliter samples

dx.doi.org/10.1021/la200649n |*Langmuir* 2011, 27, 6534–6540

with SPRI. This methodology can be used to rapidly fabricate DNA and RNA microarrays for SPRI detection of target nucleic acids and proteins in small volumes, and should be easily extendable to protein and antibody microarrays as well. The small volume format is important for applications that require rapid biosensing from limited amounts of sample, and also for samples that are highly susceptible to contamination. Additional experiments that used RNase-H amplified detection of ssDNA with ssRNA microarrays in the small volume microchips were shown to be extremely fast (perhaps uniquely so) at detecting zeptomoles of target DNA: a measurable SPRI signal was obtained after only 200s even at femtomolar concentrations of target molecules. Microarray bioaffinity detection methods that measure the accumulation of surface-bound target molecules are typically 10−100 times slower at these concentrations.[37,44] Further experiments into the exact mechanism of the RNase H amplified SPRI methodology are planned.

AUTHOR INFORMATION

Corresponding Author
*E-mail: rcorn@uci.edu.

ACKNOWLEDGMENT

This research was supported by the National Institutes of Health (GM059622), the National Science Foundation (CHE-0551935), and the DARPA Micro/Nano Fluidics Fundamentals Focus MF3 Center at UCI. RMC has a financial interest in GWC Technologies.

REFERENCES

(1) Heller, M. J. *Annu. Rev. Biomed. Eng.* **2002**, *4*, 129–153.
(2) Hennecke, G.; Scherzer, C. R. *Biomarkers Med.* **2008**, *2*, 41–53.
(3) Wolcott, M. J. *Clin. Microbiol. Rev.* **1992**, *5*, 370–386.
(4) Soifer, H. S.; Rossi, J. J.; Saetrom, P. *Mol. Ther.* **2007**, *15*, 2070–2079.
(5) Atkin, W.; Martin, J. P. *J. Natl. Cancer Inst.* **2001**, *93*, 798–799.
(6) Sehgal, A.; Gupta, S.; Parashari, A.; Sodhani, P.; Singh, V. *J. Obstet. Gynaecol.* **2009**, *29*, 583–589.
(7) Burbulis, I.; Yamaguchi, K.; Gordon, A.; Carlson, R.; Brent, R. *Nat. Methods* **2005**, *2*, 31–37.
(8) Nelson, P. T.; Baldwin, D. A.; Scearce, L. M.; Oberholtzer, J. C.; Tobias, J. W.; Mourelatos, Z. *Nat. Methods* **2004**, *1*, 155–161.
(9) Calin, G. A.; Croce, C. M. *Nat. Rev. Cancer* **2006**, *6*, 857–866.
(10) Wegner, G. J.; Wark, A. W.; Lee, H. J.; Codner, E.; Saeki, T.; Fang, S. P.; Corn, R. M. *Anal. Chem.* **2004**, *76*, 5677–5684.
(11) Homola, J. *Chem. Rev.* **2008**, *108*, 462–493.
(12) Nelson, B. P.; Grimsrud, T. E.; Liles, M. R.; Goodman, R. M.; Corn, R. M. *Anal. Chem.* **2001**, *73*, 1–7.
(13) Smith, E. A.; Erickson, M. G.; Ulijasz, A. T.; Weisblum, B.; Corn, R. M. *Langmuir* **2003**, *19*, 1486–1492.
(14) Wegner, G. J.; Lee, N. J.; Marriott, G.; Corn, R. M. *Anal. Chem.* **2003**, *75*, 4740–4746.
(15) Wegner, G. J.; Lee, H. J.; Corn, R. M. *Anal. Chem.* **2002**, *74*, 5161–5168.
(16) Smith, E. A.; Thomas, W. D.; Kiessling, L. L.; Corn, R. M. *J. Am. Chem. Soc.* **2003**, *125*, 6140–6148.
(17) Chen, Y. L.; Nguyen, A.; Niu, L. F.; Corn, R. M. *Langmuir* **2009**, *25*, 5054–5060.
(18) Gifford, L. K.; Sendroiu, I. E.; Corn, R. M.; Luptak, A. *J. Am. Chem. Soc.* **2010**, *132*, 9265–9267.
(19) Lee, H. J.; Wark, A. W.; Corn, R. M. *Analyst* **2008**, *133*, 975–983.
(20) Sendroiu, I. E.; Warner, M. E.; Corn, R. M. *Langmuir* **2009**, *25*, 11282–11284.
(21) Fang, S. P.; Lee, H. J.; Wark, A. W.; Corn, R. M. *J. Am. Chem. Soc.* **2006**, *128*, 14044–14046.
(22) Lee, H. J.; Wark, A. W.; Corn, R. M. *Analyst* **2008**, *133*, 596–601.
(23) Li, Y.; Lee, H. J.; Corn, R. M. *Anal. Chem.* **2007**, *79*, 1082–1088.
(24) Wark, A. W.; Lee, H. J.; Corn, R. M. *Angew. Chem., Int. Ed.* **2008**, *47*, 644–652.
(25) Wark, A. W.; Lee, H. J.; Qavi, A. J.; Corn, R. M. *Anal. Chem.* **2007**, *79*, 6697–6701.
(26) Goodrich, T. T.; Lee, H. J.; Corn, R. M. *J. Am. Chem. Soc.* **2004**, *126*, 4086–4087.
(27) Goodrich, T. T.; Lee, H. J.; Corn, R. M. *Anal. Chem.* **2004**, *76*, 6173–6178.
(28) Lee, H. J.; Goodrich, T. T.; Corn, R. M. *Anal. Chem.* **2001**, *73*, 5525–5531.
(29) Li, Y.; Lee, H. J.; Corn, R. M. *Nucleic Acids Res.* **2006**, *34*, 6416–6424.
(30) McDonald, J. C.; Duffy, D. C.; Anderson, J. R.; Chiu, D. T.; Wu, H.; Schueller, O. J. A.; Whitesides, G. M. *Electrophoresis* **2000**, *21*, 27–40.
(31) Meyer, R. R.; Laine, P. S. *Microbiol. Mol. Biol. Rev.* **1990**, *54*, 342–380.
(32) Bunka, D. H. J.; Stockley, P. G. *Nat. Rev. Microbiol.* **2006**, *4*, 588–596.
(33) Tasset, D. M.; Kubik, M. F.; Steiner, W. *J. Mol. Biol.* **1997**, *272*, 688–698.
(34) Gubler, U.; Hoffman, B. J. *Gene* **1983**, *25*, 263–269.
(35) Doniskeller, H. *Nucleic Acids Res.* **1979**, *7*, 179–192.
(36) Lee, H. J.; Wark, A. W.; Corn, R. M. *Langmuir* **2006**, *22*, 5241–5250.
(37) Yao, D. F.; Yu, F.; Kim, J. Y.; Scholz, J.; Nielsen, P. E.; Sinner, E. K.; Knoll, W. *Nucleic Acids Res.* **2004**, *32*, e177.
(38) Knoll, W.; Kasry, A.; Liu, J.; Neumann, T.; Niu, L.; Park, H.; Paulsen, H.; Robelek, R.; Yao, D.; Yu, F. In *Handbook of Surface Plasmon Resonance*; Schasfoort, R. B. M., Tudos, A. J., Eds.; The Royal Society of Chemistry: Cambridge, U.K., 2008; pp 275−312.
(39) Gedig, E. T. In *Hand book of Surface Plasmon Resonance*; Schasfoort, R. B. M., Tudos, A. J., Eds.; The Royal Society of Chemistry: Cambridge, U.K., 2008; pp 173−220.
(40) Lee, H. J.; Wark, A. W.; Goodrich, T. T.; Fang, S. P.; Corn, R. M. *Langmuir* **2005**, *21*, 4050–4057.
(41) Wark, A. W.; Lee, H. J.; Corn, R. M. *Anal. Chem.* **2005**, *77*, 3904–3907.
(42) Kankare, J.; Vinokurov, I. A. *Langmuir* **1999**, *15*, 5591–5599.
(43) Lukacs, G. L.; Haggie, P.; Seksek, O.; Lechardeur, D.; Freedman, N.; Verkman, A. S. *J. Biol. Chem.* **2000**, *275*, 1625–1629.
(44) Sendroiu, I. E.; Gifford, L. K.; Luptak, A.; Corn, R. M. *J. Am. Chem. Soc.* **2011**, *133*, 4271–4273.